Nanostructured Materials Generated by High-Intensity Ultrasound: Sonochemical Synthesis and Catalytic Studies

Kenneth S. Suslick,* Taeghwan Hyeon, and Mingming Fang

School of Chemical Sciences, University of Illinois at Urbana−Champaign, 505 S. Mathews Ave., Urbana, Illinois 61801

Received January 29, 1996. Revised Manuscript Received May 22, 1996[⊗]

The sonochemical decomposition of volatile organometallic compounds produces high surface area solids that consist of agglomerates of nanometer clusters. For iron pentacarbonyl and tricarbonylnitrosylcobalt, nanostructured metals and alloys are formed; for molybdenum hexacarbonyl, the metal carbide is produced. These sonochemically produced nanostructured solids are active heterogeneous catalysts for hydrocarbon re-forming and CO hydrogenation. The sonochemical synthesis, characterization, and catalytic studies will be discussed in this review.

Introduction

Nanostructured materials have been intensively studied in recent years because the physical properties of these materials are often quite different from those of the bulk.[1−4] A variety of chemical and physical preparative methods have been developed to produce materials with nanometer structure. Gas-phase techniques for the production of nanostructured metals include molten metal evaporation to produce a supersaturated metal vapor and subsequent condensation with inert gas[5−7] and metal vapor synthesis with trapping of solvated metal clusters in alkane solvents at low temperature.[8−10] A variety of solution chemical reduction methods has also been applied to make nanostructured materials; alkali-metal borohydrides,[11−13] alkalides, and electrides[14,15] have each been used to reduce metal halides to produce nanoscale metals. Thermal decomposition and laser pyrolysis of organometallic compounds have been recently used to generate nanostructured metals.[16,17] In addition, colloid chemical methods generating nanostructured materials were reviewed recently by Fendler and Meldrum.[18] And of course, the synthesis of conventional heterogeneous catalysts on oxide supports can also produce high dispersions.[19] To this range of techniques, we have added the sonochemical reactions of volatile organometallics as a general approach to the synthesis of nanophase materials.

The chemical effects of ultrasound do not come from a direct interaction between the sound field and molecular species. Sonochemistry arises from acoustic cavitation: the formation, growth, and implosive collapse of bubbles within a liquid.[20] The collapsing bubbles generate localized hot spots. This local heating produces a wide range of high-temperature and high-pressure chemistry as well as the emission of light (i.e., sonoluminescence). The conditions formed in these hot spots have been experimentally determined to have transient temperatures of ∼5000 K, pressures of ∼1800 atm, and cooling rates in excess of 10^{10} K/s.[21,22] Using these extreme conditions, we have produced a variety of nanostructured and often amorphous metals, alloys, and carbides and examined their catalytic activity.[23−31] Volatile organometallic compounds decompose inside a collapsing bubble, and the resulting metal atoms agglomerate to form nanostructured materials.

[⊗] Abstract published in *Advance ACS Abstracts,* July 15, 1996.

(1) Weller, H. *Adv. Mater.* **1993**, *5*, 88.
(2) Ozin, G. A. *Adv. Mater.* **1992**, *4*, 612.
(3) Gleiter, H. *Adv. Mater.* **1992**, *4*, 474.
(4) Chorley, R. W.; Lednor, P. W. *Adv. Mater.* **1991**, *3*, 474.
(5) Agata, M.; Kurase, H.; Hayashi, S.; Yamamoto, K. *Solid State Comm.* **1990**, *76*, 1061.
(6) Paperfthymiou, V.; Kosticas, A.; Simopoulos, A. *J. Appl. Phys.* **1990**, *67*, 4487.
(7) Hahn, H.; Averback, R. S. *J. Appl. Phys.* **1990**, *67*, 1113.
(8) Davis, S. C. ; Klabunde, K. J. *Chem. Rev.* **1982**, *82*, 152.
(9) Klabunde, K. J.; Li, Y.-X.; Tan, B.-J. *Chem. Mater.* **1991**, *3*, 30.
(10) Klabunde, K. J.; Zhang, D.; Glavee, G. N.; Sorensen, C. M. *Chem. Mater.* **1994**, *6*, 784.
(11) Bönnemann, H.; Brijoux, W.; Brinkmann, R.; Joussen, T. *Angew. Chem., Int. Ed. Engl.* **1990**, *29*, 273.
(12) Bönnemann, H.; Brijoux, W.; Brinkmann; Dinjus, E.; Joussen, T.; Korall, B. *Angew. Chem., Int. Ed. Engl.* **1991**, *30*, 1312.
(13) Zeng, D.; Hampden-Smith, M. J. *Chem. Mater.* **1993**, *5*, 681.
(14) Tsai, K.-L.; Dye, J. L. *J. Am. Chem. Soc.* **1991**, *113*, 1650.
(15) Tsai, K.-L.; Dye, J. L. *Chem. Mater.* **1993**, *5*, 540.
(16) Lisitsyn, A. S.; Golovin, A. V.; Chuvilin, A. L.; Kuznetsov, V. L.; Romanenko, A. V.; Danilyuk, A. F.; Yermakov, Y. I. *Appl. Catal.* **1989**, *55*, 235.
(17) (a) Rice, G. W. *ACS Symp. Ser.* **1993**, *530*, 273. (b) Chaiken, J. *Chem. Ind.* **1993**, 751.
(18) Fendler, J. H.; Meldrum, F. C. *Adv. Mater.* **1995**, *7*, 607.
(19) (a) Satterfield, C. N. *Heterogeneous Catalysis in Industrial Practice*, 2nd ed.; McGraw-Hill: New York, 1991. (b) Twigg, M. V. *Catalyst Handbook*, 2nd ed.; Wolfe Publishing: London, 1989. (c) Stiles, A. B. *Catalyst Manufacture: Laboratory and Commercial Preparations*; Dekker: New York, 1983.
(20) Suslick, K. S. In *Ultrasound: Its Chemical, Physical, and Biological Effects*; Suslick, K. S., Ed.; VCH Press: New York, 1988; p 123.
(21) Suslick, K. S. *Science* **1990**, *247*, 1439.
(22) Flint, E. B; Suslick, K. S. *Science* **1991**, *253*, 1397.
(23) Suslick, K. S. *MRS Bull.* **1995**, *20*, 29.
(24) Suslick, K. S. Ultrasound: Applications to Materials Chemistry. In *Encyclopedia of Materials Science and Engineering*; Cahn, R. W., Ed.; Pergamon Press: Oxford, 1993; 3rd Suppl., pp 2093−2098.
(25) Suslick, K. S.; Hyeon, T.; Fang, M; Cichowlas, A. A. *Mater. Sci. Eng. A* **1995**, *204*, 186.
(26) Fang, M. Catalytic and Magnetic Properties of Nanostructured Materials Generated by Ultrasound. Ph.D. Thesis, University of Illinois at Urbana−Champaign, 1995.
(27) (a) Suslick, K. S.; Choe, S. B.; Cichowlas, A. A.; Grinstaff, M. W. *Nature* **1991**, *353*, 414. (b) Grinstaff, M. W.; Cichowlas, A. A.; Choe, S. B.; Suslick, K. S. *Ultrasonics* **1992**, *30*, 168.
(28) Grinstaff, M. W.; Salamon, M. B.; Suslick, K. S. *Phys. Rev. B* **1993**, *48*, 269.

S0897-4756(96)00056-7 CCC: $12.00

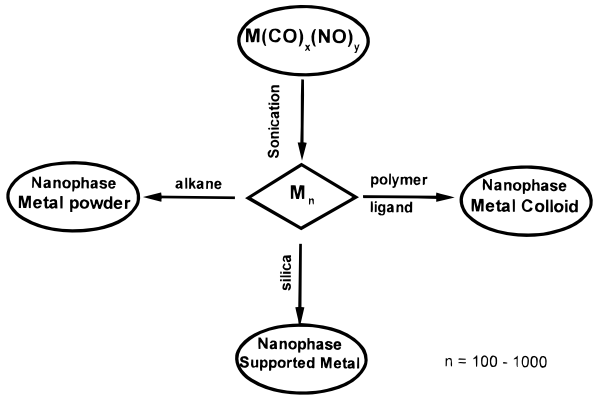

Figure 1. Sonochemical synthesis of various forms of nanostructured materials.

Sonochemical decomposition rates for volatile organometallic compounds depend on a variety of experimental parameters such as vapor pressure of precursors, solvent vapor pressure, and ambient gas. To achieve high sonochemical yields, the precursors should be highly volatile since the primary sonochemical reaction site is the vapor inside the cavitating bubbles.[32] So that decomposition takes place only during cavitation, thermal stability is also important. In addition, the solvent vapor pressure should be low at the sonication temperature, because significant solvent vapor inside the bubble reduces the bubble collapse efficiency.[20]

Our sonochemical synthesis of nanostructured materials is also extremely versatile: various forms of nanophase materials can be generated simply by changing the reaction medium (Figure 1). When precursors are sonicated in high-boiling alkanes, nanostructured metal powders are formed. If sonication occurs in the presence of a bulky or polymeric ligand (e.g., poly(vinylpyrrolidone) (PVP)), stable nanophase metal colloids are created. A transmission electron micrograph of the nanocolloid Fe/PVP is shown in Figure 2. Sonication of the precursor in the presence of an inorganic support (silica or alumina) provides an alternative means of trapping the nanometer clusters. These nanoparticles trapped upon these supports produce active supported heterogeneous catalysts. To demonstrate the utility of sonochemistry for nanostructured materials preparation, we will examine here the sonochemical synthesis and heterogeneous catalytic studies of nanostructured amorphous iron, nanostructured Fe on silica, nanophase Fe−Co alloys, and nanostructured Mo_2C.

Experimental Details

General Procedures. All manipulations for the preparation of samples were performed using Schlenk vacuum line and inert-atmosphere box (Vacuum Atmospheres, <1 ppm O_2) techniques. Pentane was distilled over sodium/benzophenone.

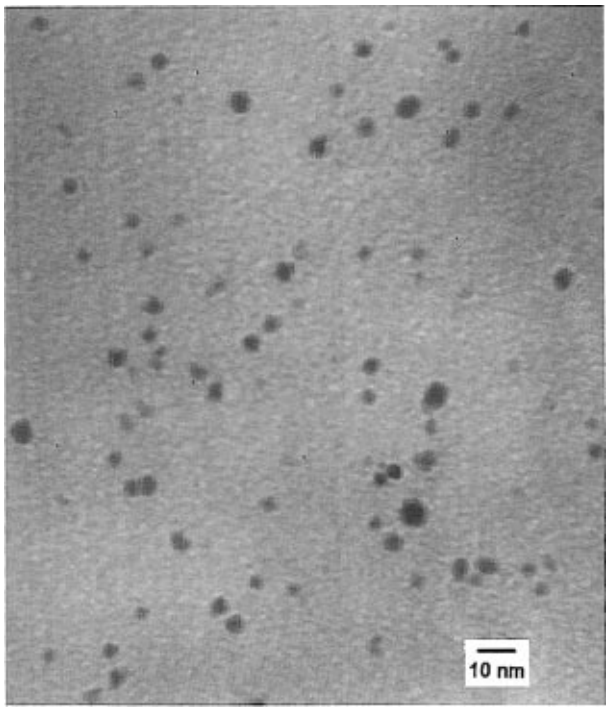

Figure 2. Transmission electron micrograph of nanostructured Fe colloid sonochemically prepared and stabilized by poly(vinylpyrrolidone), obtained on Phillips 420 electron microscope.

Decane and hexadecane were distilled over sodium. Ultrasonic irradiation was accomplished with a high-intensity ultrasonic probe (Sonic and Materials, model VC-600, 1 cm diameter Ti horn, 20 kHz, 100 Wcm^{-2}).

X-ray powder diffraction data were collected on a Rigaku D-max diffractometer using Cu Kα radiation ($\lambda = 1.5418$ Å). Scanning electron micrographs were taken on a Hitachi S800 electron microscope. Transmission electron micrographs were taken on a Phillips CM-12 electron microscope. Samples for elemental analysis were submitted in sealed vials without exposure to air.

Synthesis of Nanostructured Catalysts by Sonochemical Decomposition. For the synthesis of nanostructured Fe, Co, and Fe−Co alloy materials, solutions containing various relative concentrations of $Fe(CO)_5$ and $Co(CO)_3(NO)$ were irradiated in dry decane at 0 °C with a high-intensity ultrasonic probe for 3 h under argon. The resulting black powders were filtered and washed with dry pentane in the glovebox.

For the preparation of nanostructured Fe/SiO_2 catalysts, silica gel (Universal Scientific Incorporated chemicals, 63−100 mesh) was pretreated at 450 °C under vacuum (1×10^{-5} Torr) for 10 h before use. To this, a 0.1 M solution of $Fe(CO)_5$ in dry decane was added, in which the vapor pressure of $Fe(CO)_5$ was roughly 3 Torr at 20 °C. The slurry was then irradiated at 20 °C with a high-intensity ultrasonic probe for 3 h under argon. The resulting black powder was filtered and washed with dry pentane in an inert-atmosphere box.

Conventional silica-supported crystalline iron catalysts were prepared using the usual incipient wetness impregnation method by dissolving $Fe(NO_3)_3 \cdot 9H_2O$ in an aqueous solution containing silica gel.[33] These samples were dried at 220 °C for 12 h and calcined at 450 °C under an O_2 flow for 1 h. Reduction of iron supported on silica was carried out in a flow of hydrogen at 200 °C for 1 h, at 300 °C for 1 h, and finally at 450 °C for 2 h.

The nanostructured molybdenum carbide catalyst was prepared by ultrasonic irradiation of a slurry of molybdenum hexacarbonyl (1 g of $Mo(CO)_6$ in 50 mL of hexadecane) at 90 °C for 3 h under argon. Hexadecane was chosen as a solvent

(29) Suslick, K. S.; Hyeon, T.; Fang, M.; Cichowlas, A. A. *Molecularly Designed Nanostructured Materials*; MRS Symp. Proc., Vol. 351; Gonsalves, K. E., Chow, G. M., Xiao, T. O., Cammarata, R.C., Eds. Materials Research Society: Pittsburgh, 1994; pp 201−206.

(30) Suslick, K. S.; Fang, M.; Hyeon, T.; Cichowlas, A. A. *Molecularly Designed Nanostructured Materials*; MRS Symp. Proc., Vol. 351; Gonsalves, K. E., Chow, G. M., Xiao, T. O., Cammarata, R.C., Eds. Materials Research Society: Pittsburgh, 1994; pp. 443−448.

(31) Hyeon, T.; Fang, M; Suslick, K. S. *J. Am. Chem. Soc.* **1996**, *118*, 5492.

(32) Suslick, K. S.; Cline, Jr., R. E.; Hammerton, D. A. *J. Am. Chem. Soc.* **1986**, *106*, 5641.

(33) Bianchi, D.; Tan, L. M.; Borcar, S.; Bennett, C. O. *J. Catal.* **1983**, *84*, 358.

because its vapor pressure is low at the sonication temperature. The black powder was filtered inside a drybox and washed several times with purified, degassed pentane.

Catalytic Studies. A quartz reactor was used for both adsorption and gas−solid catalytic studies. The catalysts were transferred from an inert atmosphere box to the catalytic rig without exposure to air. Surface areas were calculated by applying the BET equation to the N_2 adsorption isotherm measured at 77 K. The gas products obtained during the temperature-programmed desorption (TPD) and temperature-programmed reduction (TPR) experiments were analyzed by a quadrupole mass spectrometer (Spectra Instruments). The catalytic reaction products were analyzed by gas chromatography (Hewlett-Packard 5730A) on an *n*-octane/Porasil C column with a flame ionization detector. Hydrogen (99.99%, Linde), methane (99.97%, Matheson), and CO (99.0+%, Linde) were further purified through 4A molecular sieves and Oxy-traps (Alltech). Cyclohexane (99+%, Fisher) was dried over molecular sieves prior to use.

Dehydrogenation and hydrogenolysis of cyclohexane were conducted by flowing a gas mixture of H_2 and cyclohexane at 1 atm through the catalysts at various reaction temperatures. In all cases, total conversions (dehydrogenation and hydrogenolysis) were kept under 10% to minimize complications due to heat and mass transfer and secondary reactions of the primary products. A digital mass flow controller (MKS, Inc.) maintained a constant flow of hydrogen (30 cm^3/min) to carry cyclohexane vapor at a constant partial pressure of 0.09 atm through the catalyst bed. The cyclohexane reaction products (benzene from dehydrogenation and aliphatic hydrocarbons from hydrogenolysis) were analyzed with a gas chromatograph (Hewlett-Packard 5730A) equipped with an *n*-octane/Porasil C column and a flame ionization detector (FID). Details of space velocity considerations and the analysis of experimental data are described elsewhere.[26]

The Fischer−Tropsch synthesis (FTS) involves CO hydrogenation to form hydrocarbons. Activity and selectivity of FTS were measured in the temperature range between 200 and 300 °C and under 1 atm pressure. Total conversions (in terms of turnover number of CO molecules converted per catalytic site per second) were kept less than 10% to minimize complications due to heat and mass transfer. The $CO/H_2/Ar$ feed gas for this reaction (99.99+%, Linde) was further purified by passing through a molecular sieve trap and a Oxy-trap from Alltech. The feed gas contained 69.5% H_2, 20.1% CO, and 10.4% Ar in volume. The flow rate was controlled by a digital mass flow controller (usually at 15 cm^3/min). The reaction products were analyzed by the GC equipped with a Porapak Q column and a Carbosieve G column and a combination of flame ionization detector (FID) and the thermal conductivity detector (TCD).

The total conversion of this reaction was calculated using the following expression:

$$\text{CO conversion, \%} = \frac{(\text{CO/Ar})_{\text{feed}} - (\text{CO/Ar})_{\text{product}}}{(\text{CO/Ar})_{\text{feed}}} \times 100\%$$

Argon was used as an internal standard for the calculation. CO, Ar, CH_4, and CO_2 were analyzed by using the Carbosieve G column and the TCD. Since different compounds have different TCD responses, correction factors were included in the calculations.

Results and Discussion

Synthesis of Amorphous Nanostructured Iron. Sonication of 1 M iron pentacarbonyl in decane at 0 °C under argon flowing yielded a dull black powder. Elemental analysis of the powder, after heating at 100 °C under vacuum to remove residual solvent, showed it to be >96% iron by weight, with trace amounts of carbon (<3%) and oxygen (1%, by difference), presumably from the decomposition of alkane solvent or carbon monoxide during ultrasonic irradiation. Scanning electron micrographs revealed the powder is agglomerates of 20 nm particles (Figure 3). Transmission electron micrographs further indicated that these 20 nm particles consist of smaller 4−6 nm particles.

The amorphous nature of the iron powder was confirmed by several different techniques, including scanning electron microscopy, differential scanning calorimetry, electron microdiffraction, and X-ray powder diffraction. Initial X-ray powder diffraction showed no diffraction peak; after heat treatment under helium at 350 °C the diffraction lines characteristic of bcc iron metal (*d* spacings of 2.03, 1.43, 1.17, and 1.04 Å) are observed (Figure 4). Electron microdiffraction revealed a diffuse ring pattern, characteristic of amorphous materials. Differential scanning calorimetry also shows one exothermic irreversible disorder−order transition temperature at 308 °C. The amorphous metal formation results from the extremely high cooling rate during acoustic cavitation.[27]

Magnetic studies showed that the amorphous nanostructured iron is a soft ferromagnetic with a saturation magnetization of 173 EMU/g and a Curie temperature in excess of 580 K.[28] The catalytic activity of the amorphous nanostructured iron was tested for the Fischer−Tropsch process (hydrogenation of CO). The catalytic conversion of carbon monoxide to low molecular weight alkanes occurred at a very low temperature (200 °C). The nanostructured iron was roughly 10 times more active (per gram) than the 5 μm commercial iron powder, in part because of higher surface area.

Synthesis and Catalytic Studies of Nanostructured Silica-Supported Fe. Ultrasonic irradiation of decane solutions of iron pentacarbonyl ($Fe(CO)_5$) in the presence of silica gel produces a silica-supported amorphous nanostructured iron. The iron loading on the SiO_2 can be easily varied by changing the initial concentration of the $Fe(CO)_5$ solution. Elemental analysis reveals Fe, Si, O, and a trace amount of carbon (<1%) to be present.

The amorphous nature of these supported iron particles has been confirmed by several different techniques, including differential scanning calorimetry (DSC), X-ray powder diffraction, and electron-beam microdiffraction. Differential scanning calorimetry shows one irreversible exothermic transition at 335 °C corresponding to a disorder−order transition (i.e., crystallization) of the amorphous iron. X-ray powder diffraction shows no diffraction peaks from the initial products. After heat treatment under He at 400 °C for 4 h (sufficient to induce crystallization), the lines characteristic of α-Fe metal (*d* spacings of 2.03, 1.43, 1.17, and 1.04 Å) are observed, no peaks can be attributed to iron oxide, iron carbide, or other iron-based phases. Electron microdiffraction with a transmission electron microscope confirms these observations and shows only a diffuse ring characteristic of amorphous iron particles.[25]

The transmission electron micrograph showed that the iron particles produced by sonolysis of $Fe(CO)_5$ were highly dispersed on the SiO_2 surface. The iron particles range in size from 3 to 8 nm (Figure 5). Chemisorption of CO permits the measurement of the dispersion and the average particle size of iron supported on silica surfaces.[34] The CO chemisorption measurement data at −78 °C on our samples gives an average iron particle size of 7 nm, in good agreement with the TEM data.

(34) Dumesic, J. A.; Topsøe, H.; Boudart, M. *J. Catal.* **1975**, *37*, 513.

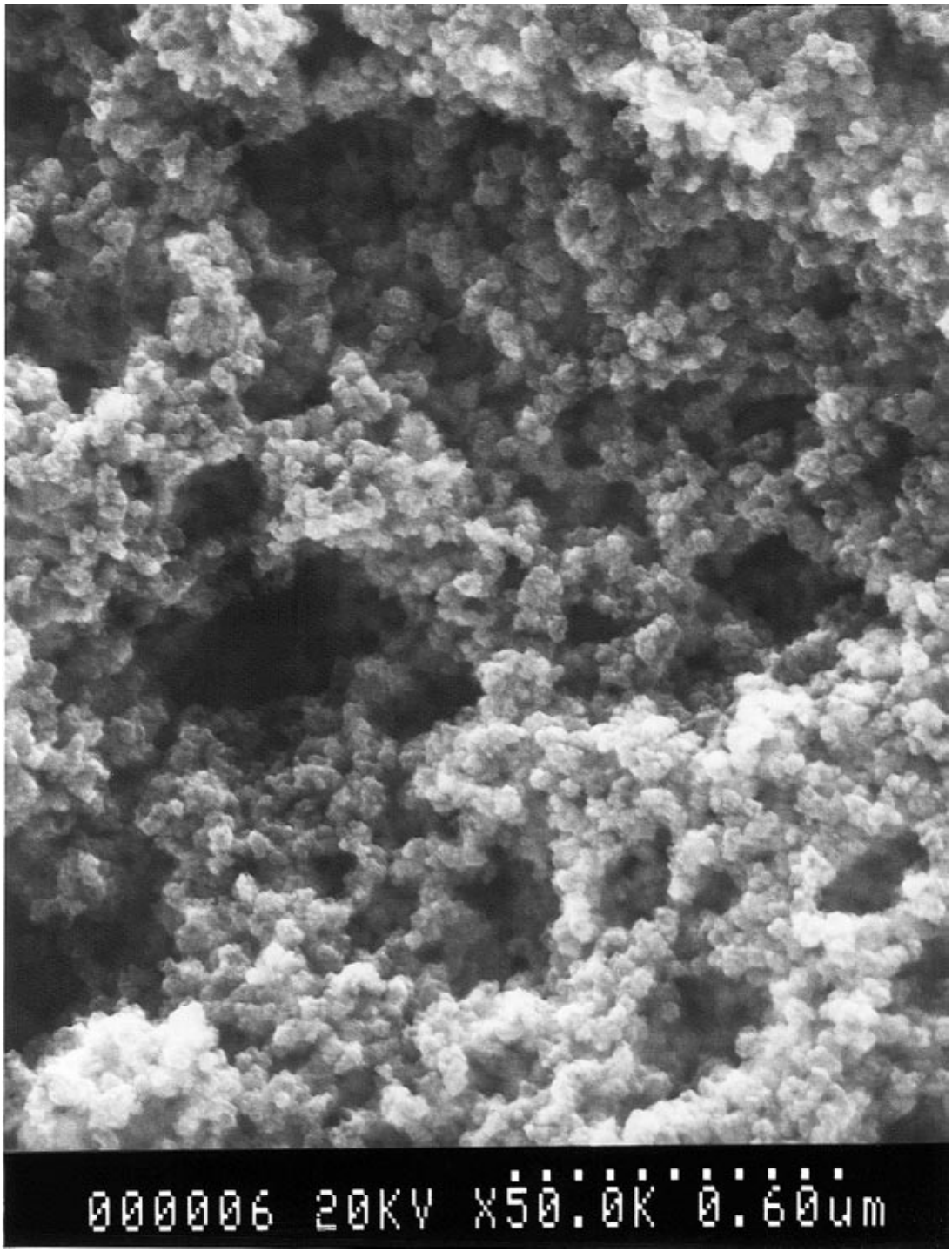

Figure 3. Scanning electron micrograph of nanostructured iron, obtained on a Hitachi S-800 electron microscope.

The catalytic activity of the silica supported nanostructured iron was probed in the commercially important Fischer−Tropsch synthesis reaction (i.e., hydrogenation of CO). Figure 6 compares the activity (in terms of turnover frequency of CO molecules converted per catalytic site per second) of silica-supported nanophase iron and conventional silica-supported iron, prepared by the incipient wetness method, as a function of temperature. These catalytic data were obtained at high iron loading and low dispersion to minimize the effects of support and dispersion. The sonochemically produced iron on silica catalyst is an order of magnitude more active than the conventional supported iron at similar loadings and dispersions. Moreover, the silica-supported nanostructured iron catalyst exhibits high activity at low temperatures (<250 °C), whereas the silica-supported conventional iron catalyst has no activity. We propose that the dramatic difference in activity between the two samples below 300 °C may be due to the amorphous nature of iron and the inherently highly defected surface formed during sonolysis of $Fe(CO)_5$ when the amorphous state of iron is preserved. At higher temperatures, the activity decreases, which may be due to iron crystallization, surface annealing, or catalyst deactivation from surface carbon deposition.

Differences in selectivities of product distributions between sonochemically prepared supported iron catalysts and conventional supported catalysts were not great. Under our conditions, the major reaction products for both catalysts are short-chain C_1 to C_4 hydro-

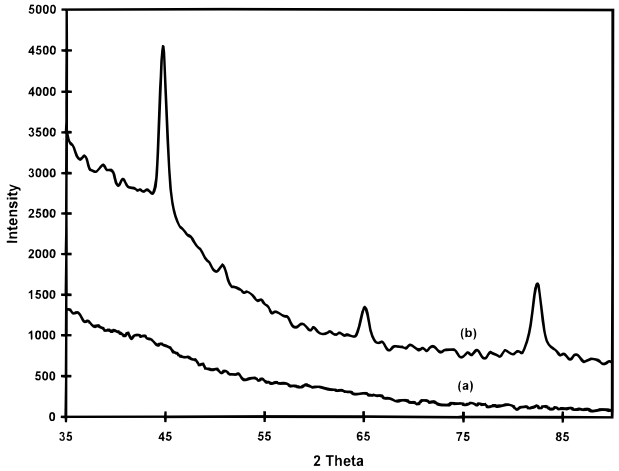

Figure 4. X-ray powder diffraction patterns of amorphous nanostructured iron powder (a) before heat treatment and (b) after crystallization at 350 °C for 6 h.

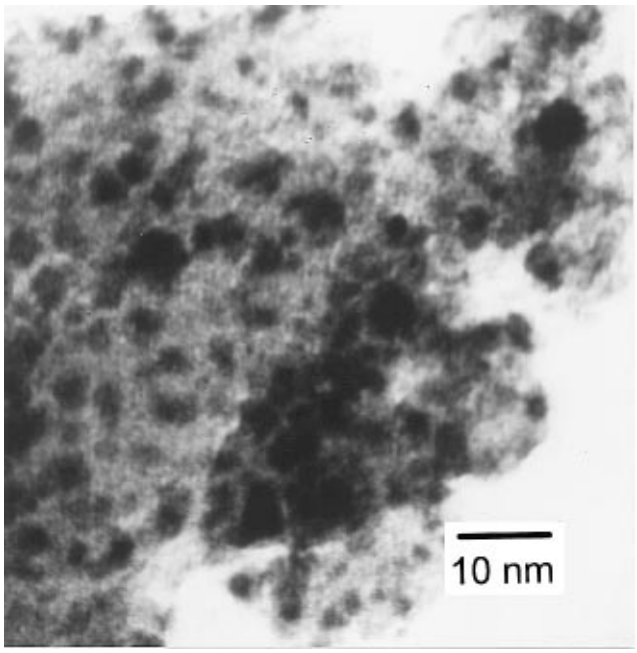

Figure 5. Transmission electron micrograph and electron microdiffraction pattern of nanometer iron particles supported on silica surface, taken on a Phillips EM400T electron microscope.

carbons and CO_2. At temperatures higher than 275 °C, the reaction product distributions are similar for both types of catalysts. At temperatures lower than 275 °C, the silica-supported iron catalyst has a higher selectivity toward long-chain hydrocarbons (C_{5+}), whereas the conventional supported iron shows no activity at those temperatures.

Synthesis and Catalytic Studies of Nanostructured Fe−Co Alloys. For a demonstration of the sonochemical synthesis of nanostructured alloys, $Fe(CO)_5$ and $Co(CO)_3(NO)$ were chosen as precursors because of their high vapor pressures at modest bulk solution temperatures where they are still thermally stable. The composition of the Fe−Co alloys can be controlled simply by changing the ratio of solution concentrations of the precursors; alloy compositions ranging from pure Fe to pure Co are readily obtained.[30]

The solid-solution nature of the alloys was confirmed by TEM-EDX measurements made on different spots

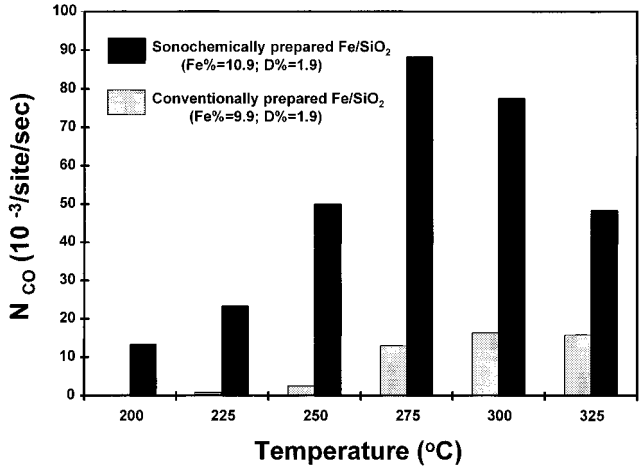

Figure 6. The catalytic activity of SiO_2 supported amorphous nanostructured iron sonochemically prepared from $Fe(CO)_5$ and SiO_2 slurry (iron loading = 10.94 wt %, and dispersion, D = 1.85%) and SiO_2-supported crystalline iron prepared by the incipient wetness method (iron loading = 9.91 wt %, D = 1.86%) as a function of temperature for Fischer−Tropsch synthesis (H_2/CO = 3.48, 1 atm, 25 °C).

of the alloy powders. The EDX results show that the alloys are homogeneous on a nanometer scale and were consistent with bulk elemental analysis. The original Fe, Co, and Fe−Co alloys produced by ultrasound are amorphous, as determined by XRD and electron-beam microdiffraction. After heat treatment under H_2 gas flow at 400 °C for 2 h, all samples underwent crystallization. The XRD results show no peaks attributable to iron/cobalt oxide, iron/cobalt carbide, or other iron/cobalt impurity phases. Pure Fe crystallizes to cubic (bcc) structure, and pure Co crystallizes to cubic (fcc) and hexagonal (hcp) mixed structures. All the alloys that we have tested so far crystallize in the bcc structure. This result is consistent with the known Fe−Co equilibrium phase diagram that strongly favors the bcc structure.[35] Elemental analysis results show that nearly pure metal and alloys are produced after H_2 treatment. SEM at high magnification indicates that these materials are porous aggregates of small clusters of 10−20 nm particles. Surface electronic structures and surface compositions of the sonochemically prepared Fe−Co alloys were also examined by using X-ray photoelectron spectroscopy (XPS). The XPS measurements have been performed on heat-treated samples before catalytic reactions. The electronic structures of the surfaces of these samples appear to be the same as the pure metals. The surface compositions of the alloys demonstrate some small enrichment of Fe over Co. Similar trends toward an iron-enriched surface have been reported by other researchers with other preparations using coprecipitation methods.[36]

Catalytic studies of the sonochemically prepared Fe−Co alloys were made for cyclohexane dehydrogenation and hydrogenolysis reactions. All catalysts were treated under H_2 gas flow at 400 °C for 2 h before the catalytic studies. While this does not alter the size of the clusters that make up the nanostructure of these materials significantly, it does cause their crystallization. H_2

(35) Nishizawa, T.; Ishida, K. *Bull. Alloy Phase Diagrams* **1984**, *5*, 250.

(36) Nakamura, M.; Wood, B. J.; Hou, P. Y.; Wise, H. In *Proc. 4th Int. Cong. on Catal., Tokyo*; Kodansha Ltd.: Tokyo, 1981; p 432.

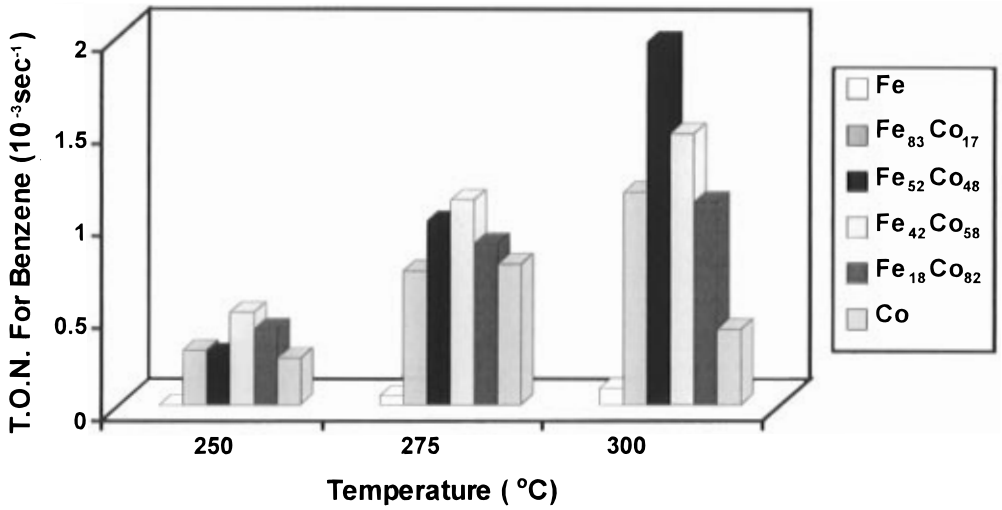

Figure 7. Catalytic activity of Fe, Co, and Fe−Co alloys for dehydrogenation of cyclohexane to benzene as a function of temperature.

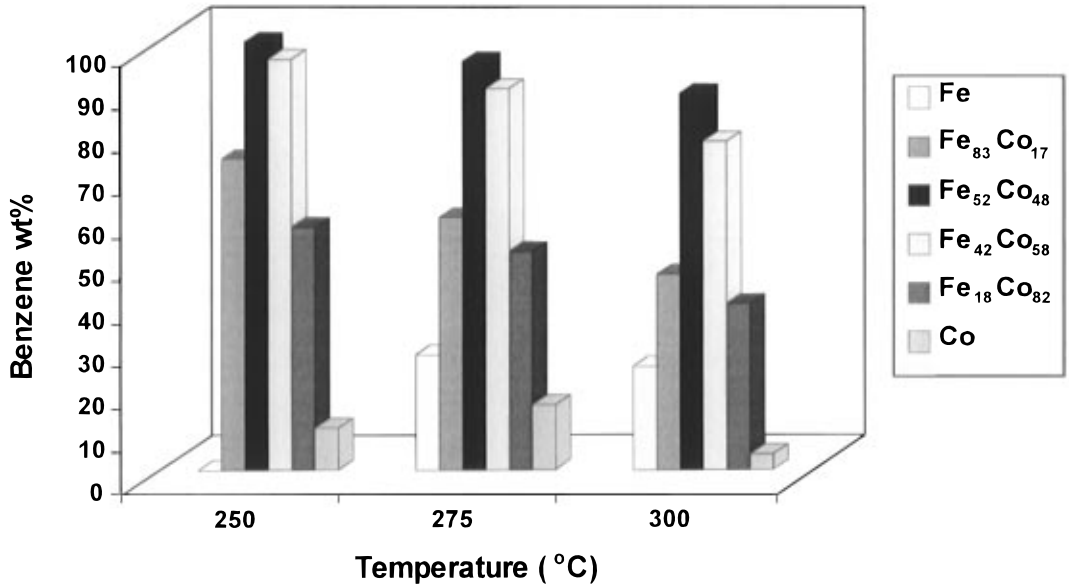

Figure 8. Catalytic selectivity of Fe, Co, and Fe−Co alloys for dehydrogenation versus hydrogenolysis of cyclohexane as a function of temperature.

treatment is necessary, however, to provide a reproducible catalytic surface. The catalytic activity (in terms of turnover frequency of cyclohexane molecules converted to benzene per surface Fe or Co atom per second) as a function of temperature is shown in Figure 7. Two kinds of products were formed during the cyclohexane reaction: benzene from the dehydrogenation reaction and aliphatic hydrocarbons (mostly methane) from the hydrogenolysis. The catalytic selectivity (in terms of the percentage of benzene among all the reaction products) as a function of temperature is shown in Figure 8. The catalytic properties of the sonochemically prepared Fe, Co, and Fe−Co alloys in the cyclohexane reaction exhibit interesting trends. First, they are all active catalysts for cyclohexane conversion: pure Co has the highest activity (albeit primarily for hydrogenolysis), pure Fe has the lowest activity, and Fe−Co alloys have intermediate activity between pure Fe and pure Co. Second, Fe−Co alloys generate much more dehydrogenation product (benzene) than pure Fe or Co. Third, the 1:1 Fe/Co alloy has both much higher dehydrogenation activities and selectivities at all reaction temperatures (250−300 °C) than the other alloys or pure metals. In the best cases, the selectivity for dehydrogenation approaches 100%. While we do not yet understand the origin of this improved selectivity in these systems, for other bimetallic catalysts for dehydrogenation of cyclohexane involving Pt, selectivity is similarly improved in the alloys.[37,38]

Synthesis and Catalytic Studies of Nanostructured Molybdenum Carbide. Recently, molybdenum and tungsten carbides have been explored as heterogeneous catalysts because of the similarity in activity that these carbides share with platinum group metals.[39−41] For catalytic applications, high surface area materials are generally needed. The preparation of interstitial carbides of molybdenum and tungsten with high surface

(37) Sinfelt, J. H. *Bimetallic Catalysts: Discoveries, Concepts, and Applications*; J. Wiley & Sons: New York, 1983; pp 18−31.
(38) Klabunde, K. J.; Li, Y.-X. *Selectivity in Catalysis*; Davis, M. E., Suib, S. L., Eds.; American Chemical Society: Washington, D. C., 1993; pp 88−108 and references therein.
(39) Ranhotra, G. S.; Haddix, G. W.; Bell, A. T. ; Reimer, J. A. *J. Catal.* **1987**, *108*, 40.
(40) Lee, J. S.; Oyama, S. T.; Boudart, M. *J. Catal.* **1990**, *125*, 157.
(41) Ledoux, M. J.; Pham-Huu, C.; Guille, J.; Dunlop, H. *J. Catal.* **1992**, *134*, 383.

areas, however, is very difficult. Boudart and Volpe prepared carbides of molybdenum and tungsten with high surface areas by the temperature-programmed carburization of the corresponding nitrides.[42] We have developed a simple sonochemical synthesis of nanophase molybdenum carbide from the ultrasonic irradiation of molybdenum hexacarbonyl.

Sonochemical decomposition of molybdenum hexacarbonyl in hexadecane produced a black powder. X-ray powder diffraction (XRD) showed extremely broad peaks centered at *d* spacings of 2.4, 1.5, and 1.3 Å, which do not match the body-centered cubic (bcc) lines of molybdenum metal. After heat treatment at 450 °C under helium flow for 12 h, sharper peaks in the XRD were observed at *d* spacing values of 2.39, 1.49, and 1.27 Å, which match very well with face-centered cubic (fcc) molybdenum carbide, Mo_2C. Elemental analysis also confirmed the stoichiometry of 2Mo/C, but with some oxygen as discussed below. The formation of molybdenum carbide can be explained by the disproportionation of carbon monoxide on the active metal surface to form carbon and carbon dioxide.[43]

The synthesis of Mo_2C is particularly prone to substantial oxygen contamination.[44] Even after heat treatment at 450 °C under helium, oxygen was still present at about 4 wt %. Since the presence of oxygen could poison the catalytic activity, it was removed before catalysis by heating in a flowing 1:1 CH_4/H_2 mixture at 300 °C for 1 h, then at 400 °C for 1 h, and finally at 500 °C for 48 h. The flow rate of the CH_4/H_2 mixture was 27.5 cm^3 (STP)/min. After this carburization, excess carbon, hydrogen and oxygen had been largely removed. The elemental analysis results showed that the sample had a stoichiometry of $Mo_2C_{1.02}$ with less than 0.09 wt % oxygen (by difference) and <0.02 wt % hydrogen. The XRD was essentially unchanged by carburization.

The scanning electron micrographs showed that the surface is extremely porous. Before carburization, high-resolution transmission electron microscopy revealed that the material is a porous aggregate of 2 nm diameter particles (Figure 9). The particle diameter calculated from the line broadening of X-ray powder diffraction was 1.6 nm.[45] Surface area, determined by BET gas adsorption isotherms was found to be 188 m^2/g. After carburization, the material remains a porous aggregate with particle size increasing slightly to 3 nm in diameter; the BET surface area decreased to 130 m^2/g.

The catalytic activity and selectivity of the sonochemically produced molybdenum carbide was examined for the dehydrogenation versus hydrogenolysis of cyclohexane with a flow catalytic microreactor. This reaction was chosen because the suppression of hydrocarbon cracking during dehydrogenation remains an important challenge for non-platinum catalysts.[46,47] To compare the catalytic properties, commercial ultrafine powders of platinum and ruthenium (Aldrich Chemicals Co., 0.27−0.47 μm diameter) were also used under identical conditions, after heating at 400 °C for 3 h under H_2 flow to remove surface contaminants. Figure 10 shows the catalytic activity (in terms of turnover frequency of cyclohexane molecules converted per second per gram of catalyst) as a function of temperature for the Mo_2C sample pretreated under CH_4/H_2 at 500 °C for 48 h compared to commercial ultrafine platinum powder.[31]

At all reaction temperatures examined, benzene was the only product formed for both samples and their activities were comparable: no hydrogenolysis products were detected. In contrast, only hydrogenolysis, mostly to methane, occurred with commercial ruthenium pow-

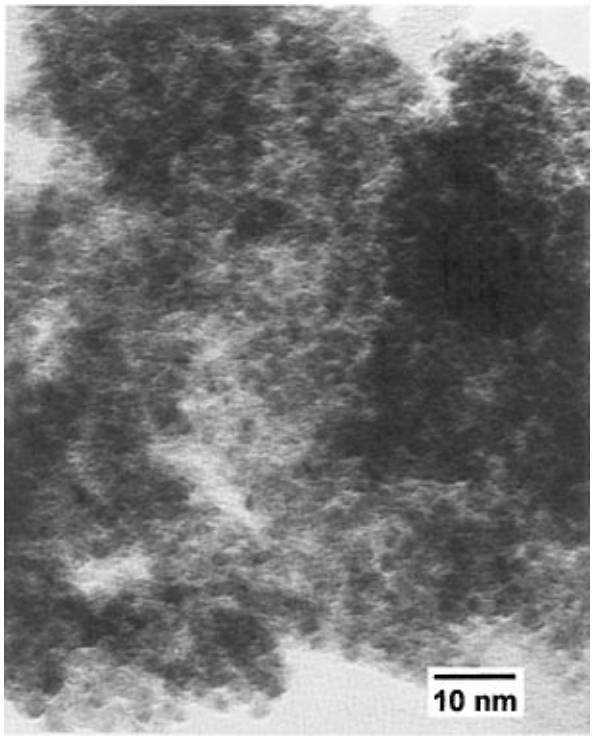

Figure 9. Transmission electron micrograph of sonochemically produced Mo_2C, obtained on a Phillips CM-12 electron microscope.

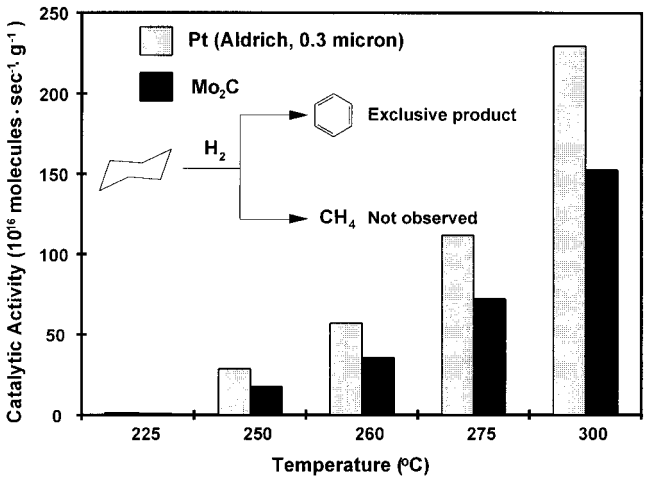

Figure 10. Catalytic activity for dehydrogenation of cyclohexane of sonochemically produced Mo_2C sample after carburization under CH_4/H_2 and commercial ultrafine platinum powder after heating under H_2. Comparisons are made on a total mass basis because cost of materials is an important concern with these catalysts. Surface areas from BET measurements are 130 m^2/g for Mo_2C and 16 m^2/g for Pt.

(42) Volpe, L.; Boudart, M *J. Solid State Chem.* **1985**, *59*, 332.
(43) Rodriguez, N. M.; Kim, M. S.; Baker, R. T. K. *J. Catal.* **1993**, *144*, 93.
(44) Ranhotra, G. S.; Haddix, G. W.; Bell, A. T.; Reimer, J. A. *J. Catal.* **1987**, *108*, 24.
(45) Cullity, B. D. *Elements of X-ray Diffraction*; Addison-Wesley: Reading, MA, 1978; p 284.
(46) Gates, B. C. *Catalytic Chemistry*; John Wiley & Sons: New York, 1992; pp 387−392.
(47) Somorjai, G. A. *Introduction to Surface Chemistry and Catalysis*; Wiley-Interscience: New York, 1994; pp 500−512.

der. The analogy has often been made that Mo_2C is similar to Ru whereas W_2C behaves like Pt.[42] These results demonstrate, however, that for dehydrogenation of alkanes, sonochemically prepared nanostructured molybdenum carbide has a selectivity similar to Pt rather than to Ru.

Conclusions

Sonochemical decomposition of volatile organometallic precursors in high-boiling solvents produces nanostructured materials in various forms with high catalytic activities. Nanometer colloids, nanoporous high surface area aggregates, and nanostructured oxide-supported catalysts can all be prepared by this general route. For example, sonication of iron pentacarbonyl with silica generated an amorphous nanostructured Fe/SiO_2 supported catalyst. This nanostructured Fe/SiO_2 catalyst showed higher catalytic activity for the Fischer−Tropsch synthesis compared to the conventional Fe/silica catalyst prepared by incipient wetness method. Sonochemical synthesis of high surface area alloys can be accomplished by the sonolysis of $Fe(CO)_5$ and $Co(CO)_3(NO)$. The sonochemically prepared Fe−Co alloys have large surface areas relative to the bulk metal even after heat treatment. We find very high catalytic activity for these Fe, Co, and Fe−Co powders for the dehydrogenation and hydrogenolysis of cyclohexane. Surprisingly, the Fe−Co alloys show very high selectivities for dehydrogenation. Finally, ultrasonic irradiation of $Mo(CO)_6$ produces aggregates of nanometer-sized clusters of face centered cubic molybdenum carbide. The material is extremely porous with a high surface area and consists of aggregates of $\approx$2 nm sized particles. The catalytic properties of molybdenum carbide generated by ultrasound reveal an active and highly selective dehydrogenation catalyst comparable to commercial ultrafine platinum powder.

Acknowledgment. This work was supported by the National Science Foundation. We thank Peggy Mochel, Vania Petrova, and the UIUC Center for Microanalysis of Materials, which is supported by the Department of Energy, for their assistance in the electron microscopic studies. We also thank Professor D. Casadonte for helpful discussions on Fe−Co alloys.

CM960056L